Available online at www.sciencedirect.com
ScienceDirect
Ceramics International 37 (2011) 3747–3754
CERAMICS INTERNATIONAL
www.elsevier.com/locate/ceramint

Short communication

Low-temperature calcination at 800 °C of alumina–zirconia nanocomposites using sugar as a gelling agent

Rifki Septawendar [a,*], Apriani Setiati [b], Suhanda Sutardi [a]

[a] Laboratory of Nano Materials, Department of Advanced Ceramics, Glass, and Enamel, Center for Ceramics, Ministry of Industry of Indonesia, Akhmad Yani 392, Bandung 40272, West Java, Indonesia
[b] Department of Ceramics and Raw Material Testing, Center for Ceramics, Ministry of Industry of Indonesia, Akhmad Yani 392, Bandung 40272, West Java, Indonesia

Received 29 March 2011; received in revised form 17 May 2011; accepted 17 May 2011
Available online 26 May 2011

Abstract

Alumina–zirconia nanocomposite powder was synthesized at a room temperature and calcined at a lower temperature than 1000 °C of about 800 °C by sugar precursor process. In the synthesis process of the nanocomposite powder, sugar was used as a gelling agent. The synthesized powder was calcined at temperatures of 800 °C, 900 °C, 1000 °C, 1100 °C, and 1200 °C for 5 h. The calcined powder was characterized by X-ray diffraction (XRD), a SYMPATEC NIMBUS particle size analysis, and transmission electron microscopy (TEM). Alumina–zirconia nanocomposites were obtained at 800 °C, where the phases formed were γ-Al_2O_3, m-ZrO_2, and t-ZrO_2. The TEM results showed that the average grain sizes of the nanocomposite were less than 25 nm in diameter. At 800 °C, a particle size analyzer measured the largest nanocomposite particles as having a size of about 40 nm, accounting for 3.49% of the total, while the most commonly sized partical was about 10 nm for 39.87%. A further phase transformation of alumina–zirconia nanocomposites was obtained at 1100 °C, where the phases formed were α-Al_2O_3, m-ZrO_2, and t-ZrO_2; the TEM results show that the average grain sizes of the nanocomposite powder were below 50 nm in diameter.

Keywords: Alumina; Zirconia; B. Nanocomposites; A. Calcination; Sugar; Precursor

1. Introduction

Alumina (Al_2O_3) shows excellent physical and chemical properties, including the highest strength among oxides, excellent abrasion resistance, heat resistance, high dielectric strength at high voltage, and high resistance to chemical attack (Table 1). Thus, these characteristics have led to the wide use of Al_2O_3 in many great applications with electronic, optical, mechanical, and biological functions [1–5]. Zirconia (ZrO_2) is another oxide material that shows excellent properties, such as high mechanical strength (compressive strength 1000–1800 MPa), high fracture toughness (8–13 MPa $m^{1/2}$), and high hardness (Vickers hardness 13–24 GPa); it is also thermally stable (m.p. 2680 °C), and chemically inert. Therefore, zirconia is frequently used as a material for structural and electrical purposes [6–8].

Composites of alumina and zirconia; in which alumina is used as a matrix, are well known as zirconia-toughened alumina (ZTA). ZTA is interesting because of its enhanced mechanical properties, such as toughness, strength, and hardness (see in Table 2). ZTA is frequently found in heat engines, rocket nozzles and cutting tools. The increased toughness of ZTA is attributed to volume and shape changes that occur during the stress-induced metastable tetragonal to monoclinic transformation of zirconia [9]. In addition to the transformation toughening associated with the t–m transformation around advancing cracks, other mechanisms; such as crack deflection, crack bridging and the presence of microcracks; may also enhance the toughness [10–14].

Nevertheless, to yield optimum strength and toughness, certain design criteria must be met by zirconia particles so that they disperse in the alumina matrix. These criteria include particle size, basic properties of the ZrO_2 particles, and ZrO_2 distribution in the alumina matrix. These factors are strongly affected by the synthesis process of the ZTA composite [5,9].

* Corresponding author. Tel.: +6285624249484.
E-mail address: rifkiseptawendar@yahoo.com (R. Septawendar).

0272-8842/$36.00
doi:10.1016/j.ceramint.2011.05.086

Table 1
Mechanical, thermal, and electrical properties of 99.8% Al_2O_3 [1,2].

Property (condition, unities)	Value
Bulk density (20 °C, g/cm^3)	3.96
Tensile strength (20 °C, MPa)	220
Bending strength (20 °C, MPa)	410
Elastic modulus (20 °C, GPa)	375
Hardness (20 °C, MPa)	137.2 93
Fracture toughness (20° C, MPa m$^{1/2}$)	4–5
Thermal expansion coefficient (10^{-6}/°C)	
25–300° C:	7.8
25–1000° C:	8.1
Thermal conductivity (20° C, W/m K)	28
Dielectric constant (1 MHz)	9.7
20 °C	$>10^{-14}$

Nanocrystalline materials show superior phase homogeneity, enhanced sinterability at a relatively low temperature and microstructures leading to unique electrical, mechanical, dielectric, magnetic and optical properties. Therefore, alumina–zirconia nanocomposites exhibit excellent chemical and physical properties compared to the composites in normal or coarse powder, due to the small particle diameter and will possess a better sintering ability [15–18].

Many synthesis methods have been proposed for alumina–zirconia nanocomposite preparation, such as sol–gel processing, the liquid precursor method, modified colloidal routes, hydrothermal processing and an injection molding [5,11,13,16,19–21]. The first three methods have been widely used for producing alumina–zirconia nanocomposites because they are versatile, show good reproducibility, and generate products with high purity and homogeneous structures.

According to previous researchers, alumina–zirconia nanocomposites form at quite high temperatures above 1000 °C [15,16]. The aims of this work are to calcine the synthesized alumina–zirconia nanocomposite powder at a lower temperature than 1000 °C of about 800 °C; and to investigate the phase transformation and crystal sizes of the alumina–zirconia nanocomposites formed. The alumina and zirconia starting materials used were the Al^{3+} cation of aluminium salt ($Al(NO_3)_3{\cdot}9H_2O$) and the Zr^{4+} cation of zirconium salt ($ZrOCl_2{\cdot}8H_2O$), which had very small ionic sizes of 0.53 nm and 0.75 nm, respectively. These cations were then coated with sugar to restrict the faster growth of crystals, thus obstructing the formation of larger particles. At a lower calcination temperature of 1000 °C, it is assumed that alumina and zirconia will form very small crystals. In this work, the calcination was conducted at temperatures from 800 °C to 1200 °C. X-ray diffraction (XRD) analysis was conducted to identify the crystalline phases and the crystallite sizes of calcined alumina–zirconia nanocomposite powder using an X-ray Phillips Pan Analytical instrument. A SYMPATEC NIMBUS particle size analysis was performed to calculate particle size distributions of the alumina–zirconia nanocomposite powder. Transmission electron microscopy (TEM) was performed using Tecnai G^2 20 Twin to verify grain morphology and sizes.

Table 2
Main properties of ZTA composites [1].

Property (condition, unities)	Value
Density (20° C.g/cm^3)	3–4
Bending strength (20° C. MPa)	300–600
Bending strength (1400° C. MPa)	100–400
Fracture toughness (20° C, MPa m$^{1/2}$)	8
Hardness (20° C, MPa)	18–23
Young's modulus	300
Thermal expansion coefficient (10^{-6}/°C)	
20–1200° C:	8
Thermal conductivity (20 °C, W/m K)	30
Thermal shock resistance	Medium
Abrasion resistance	Good

2. Experimental

2.1. Materials and instruments

Materials used in this work were aluminium nitrate nonahydrate ($Al(NO_3)_3{\cdot}9H_2O$, >98.99% purity), zirconium oxychloride octahydrate ($ZrOCl_2{\cdot}8H_2O$, 99.9% purity), 25% ammonia solution, which obtained from Merck Inc. and technical grade sugar from a local market, consisting of sucrose as a major constituent and the other organic constituents. The instruments used were an IKA dual speed mixer model RW 20 DZM with the maximum speed of 2000 rpm, a Heraus electrical furnace, a Nabertherm electrical furnace, an X-Ray Phillips PANalytical EMPYREAN with *X'Celerator detector*, a SYMPATEC NIMBUS particle size analyzer, and a TECNAI G2-200 kV Phillips transmission electron microscope.

2.2. Synthesis of alumina–zirconia nanocomposites

The precursor materials for the preparation of alumina and zirconia sols were aluminium nitrate nonahydrate, $Al(NO_3)_3{\cdot}9H_2O$ and zirconium oxychloride octahydrate, $ZrOCl_2{\cdot}8H_2O$. Single component alumina and zirconia sols were prepared separately from the respective precursor materials with the Al_2O_3:ZrO_2 weight percent ratio of 83:17. The appropriate amount of $Al(NO_3)_3{\cdot}9H_2O$ was dissolved in distilled water to give an Al^{3+} aqueous solution. The calculated quantity of zirconium oxychloride solution was also prepared. The pH of both the solutions was then adjusted, at ambient temperature, to about 7 by dropwise addition of 25% concentrated ammonia solution under vigorous stirring. The sols produced then were mixed under constant stirring at approximately 800 rpm. A solution of approximately 16% (w/v) sugar in distilled water was prepared separately. The appropriate amount of the sol mixture was then mixed with the sugar solution such that the metal salt to sugar weight ratio was maintained at 6:1 and; stirred constantly at approximately 800 rpm to give a gel. The gel was heated slowly until a concentrated yellowish brown gel was formed. The concentrated gel was slowly and continuously heated while simultaneously being stirred, until the water had completely evaporated and a black concentrated gel was formed. The black

gel was then dried in an oven at 200 °C to produce black charcoal precursors. The precursors were milled in kerosene using a pot mill, for 24 h; and successfully calcined at 800–1200 °C in an electric furnace to give very fine white powders. The calcined powders were then characterized by X-ray diffraction, a SYMPATEC NIMBUS particle size analysis, and transmission electron microscopy.

3. Result and discussion

3.1. X-ray analysis

The powder XRD analysis results of which are shown in Figs. 1 and 2, shows the phase transformations of the alumina–zirconia nanocomposites occurring over 5 h at temperatures of 800 °C, 900 °C, 1000 °C, 1100 °C, and 1200 °C. According to Fig. 1, when sugar was used as a gelling agent in a water medium, zirconium salt and aluminium salt were found to transform and crystallize at a lower temperature than 1000 °C of about 800 °C, with peaks at 28.21° and 31.45° (2θ-CuKα), corresponding to the $(\bar{1}\,1\,1)$ and (1 1 1) crystal planes of the monoclinic zirconia structure; the other phases present were identified as metastable γ-alumina at diffraction angles of 37.64° (3 1 1), 45.91° (4 0 0), and 67.08° (4 4 0) and as tetragonal zirconia with a sharp peak at 30.25° (1 0 1). This result seems to be different from the findings of Chartterjee et al. [5] and Beitollahi et al. [16]. Chartterjee et al. [5] found crystallization of both the γ-Al_2O_3 and t-ZrO_2 phases occurring at the higher temperature of 1000 °C when using triethylamine (TEA) as the gelling agent in a medium of water-in-oil emulsion. At that temperature, Beitollahi et al. [16] found the formation of the t-zirconia phase along with the other alumina meta-stable phases, such as γ, δ, and θ, using PVA and sucrose as templates. Generally, the emergence of different phases may be controlled by the specific conditions of the operating process, such as the type of template, gelling agent and medium, temperature condition during preparation, etc. [15,16].

At the higher temperatures of 900 °C and 1000 °C (Fig. 1), the main peak intensities of m-ZrO_2 at 28.21° and 31.45° increased with an elevation of the calcination temperature, whereas the peak intensity of t-ZrO_2, a sharp peak at 30.25° decreased. In fact, at a temperature of 1000 °C, the peak intensity of t-ZrO_2 was low, and some of the γ-Al_2O_3 phases transformed to α-Al_2O_3 phases; this phenomenon is indicated by the remarkable intensities of the main α-Al_2O_3 difraction peaks at 25.61° (0 1 2), 35.19° (1 0 4), 43.41° (1 1 3), and 57.58° (1 0 6). Nevertheless, at temperatures of 1100 °C and 1200 °C, the existence of the t-ZrO_2 phase in the sample was at a very low level, and the γ-Al_2O_3 phase no longer existed in the sample because it had completely transformed to the α-Al_2O_3 phase. Therefore, the direct phase transformation that occurred at 1100 °C was m-ZrO_2 (high int.) + t-ZrO_2 (low int.) + γ-Al_2O_3 (very low int.) + α-Al_2O_3 (normal int.) → m-ZrO_2 (higher int.) + t-ZrO_2 (very low int.) + α-Al_2O_3 (quite high int.).

ZrO_2 has three polymorphs: $P2_1/c$ monoclinic (m), $P4_2/nmc$ tetragonal (t), and $Fm3m$ cubic (c) crystal structures, with m-zirconia being the equilibrium bulk structure at room temperature [22]. Bulk m-zirconia transforms to t- or c-ZrO_2 at 1170 °C or 2370 °C, respectively. Various attempts have been made to stabilize c- and t-ZrO_2 at room temperature by doping them with small amounts of different dopants, such as Y_2O_3,

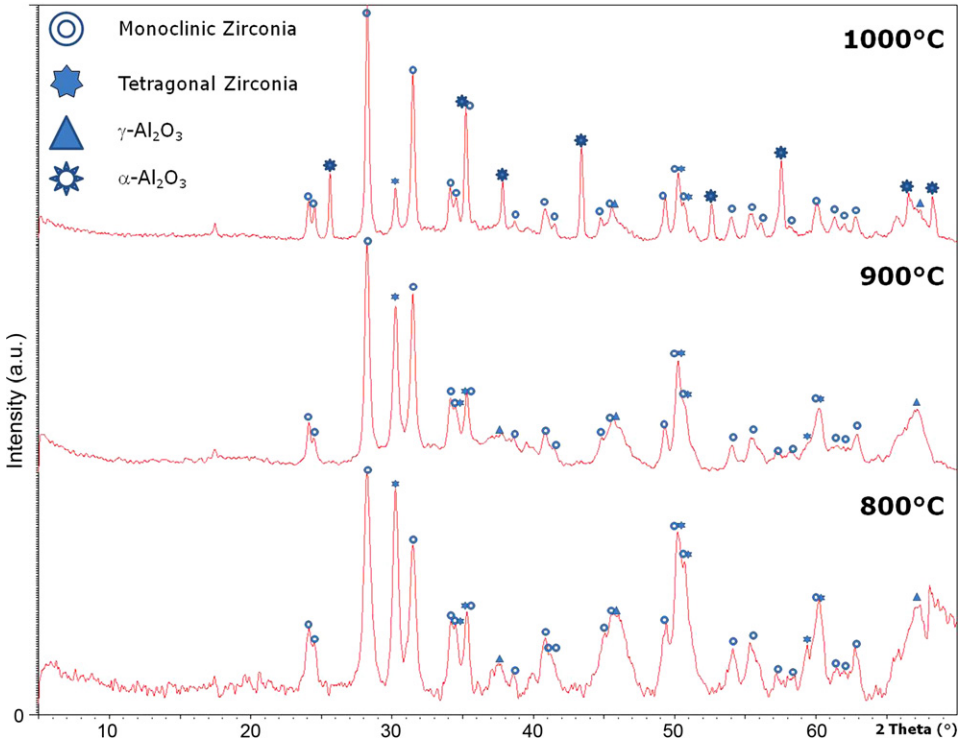

Fig. 1. XRD patterns of the alumina–zirconia nanocomposite calcined at 800 °C, 900 °C, and 1000 °C for 5 h.

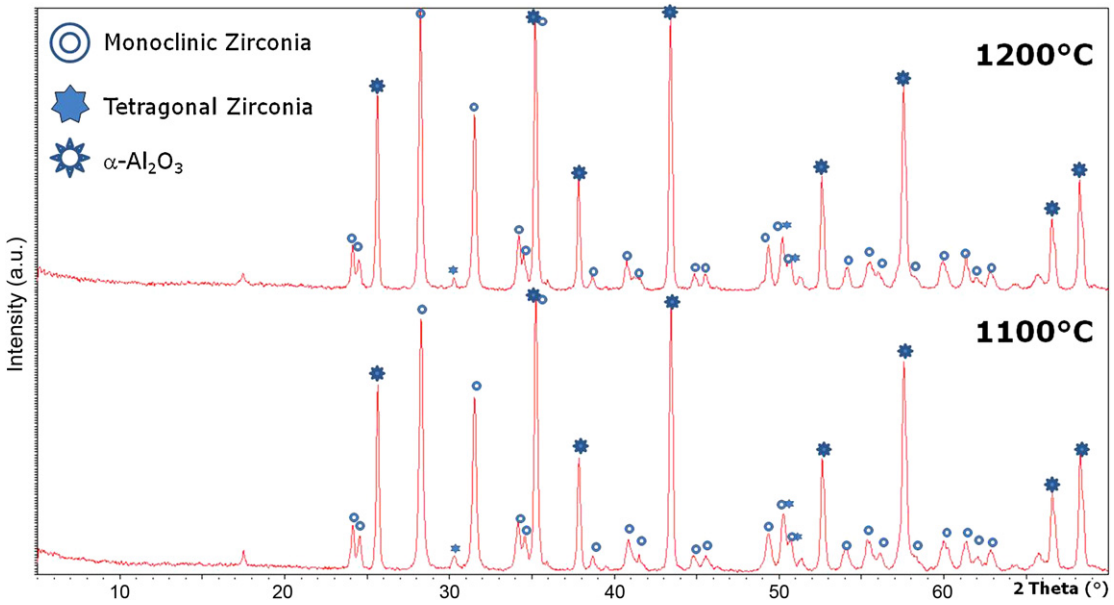

Fig. 2. XRD patterns of the alumina–zirconia nanocomposite calcined at 1100 °C and 1200 °C for 5 h.

MgO, CaO, and Al_2O_3 [23–25]. Murase et al. [23] and Beitollahi et al. [16] observed that the growth of the ZrO_2 crystallite was negligible in the presence of Al_2O_3, while a significant increase in growth was observed in pure ZrO_2 powder. This confirms the crucial effect of the presence of the matrix alumina phase on the structure and crystallite size of the zirconia phase.

Those results are slightly different from the results of the present work. As is clear from Figs. 1 and 2, the m- and t-zirconia phases were identified with similar intensities at 800 °C, and during heating treatment at the higher temperature, the intensity of m-ZrO_2 increased while the presence of t-ZrO_2 phase decreased as was significantly shown at 1200 °C. However, this finding demands further study, which is currently under way.

The preparation of alumina–zirconia nanocomposites was easier to obtain from aluminium and zirconium salts. The salts were prepared to make alumina–zirconia sols as precursor materials. The sols were prepared by adding the 25% concentrated ammonia solution to the aluminium and the zirconium solutions slowly, at ambient temperature, while stirring at a speed of 800 rpm. The sols were converted to gel by the addition of sugar. The mixing was proceeded under stirring and slow heating.

The rate of a chemical reaction depends on the following: (a) pH, (b) concentration, and (c) solution [1]. When salts are dissolved in the solution, the solution is not always neutral in reaction. This is because some of the salts interact with water; hence it is termed hydrolysis. As a result, hydrogen or hydroxyl ions remain in the solution in excess. Therefore, the solution itself is becoming acid or basic respectively. The metal salts of aluminium nitrate nonahydrate, $Al(NO_3)_3{\cdot}9H_2O$ and zirconium oxychloride octahydrate, $ZrOCl_2{\cdot}8H_2O$ are types of salts of strong acids and weak bases, when dissolved in water, produce a solution, which reacts acidic. This phenomenon is in agreement with the experimental results, where the pH of both the aluminium and zirconium solutions measured was equal to 1; both the aluminium and zirconium solutions were very acidic solutions. When a salt of aluminium nitrate is dissolved in distilled water, a hydrated aluminium ion would be produced from aqueous aluminium nitrate in the ion complex form of aluminium hexaaqua ion, where the reaction is as follows [26,27]:

$$[Al(H_2O)_6]^{3+}{}_{(aq)} + H_2O_{(l)} \rightleftharpoons [Al(H_2O)_5(OH)]^{2+}{}_{(aq)} + H_3O^{+}{}_{(aq)} \quad (1)$$

or

$$[Al(H_2O)_6]^{3+}{}_{(aq)} \rightleftharpoons [Al(H_2O)_5(OH)]^{2+}{}_{(aq)} + H^{+}{}_{(aq)} \quad (2)$$

Whereas a salt of $ZrOCl_2{\cdot}8H_2O$ is hydrolyzed in water, a tetrameric cation of $[Zr_4(OH)_8(H_2O)_{16}]^{8+}$ is formed in which there is a square of Zr^{4+} ions with two hydroxide groups bridging between Zr atoms on each side of the square and with four water molecules attached to each Zr atom [28].

The hydrolysis process of both the aluminium and zirconium solutions was accelerated with the addition of a NH_4OH catalyst. The pH of both the solutions was then adjusted, at ambient temperature, to about 7 by dropwise addition of 25% concentrated ammonia solution under vigorous stirring, until the white sols of aluminium hydroxide ($Al(OH)_3$) and zirconium hydroxide ($ZrO_2{\cdot}H_2O$ or $Zr(OH)_4$) were formed. It is noticed that the solubility of aluminium hydroxide decreased in the presence of ammonium salt (NH_4NO_3, NH_4Cl, etc.) owing the common ion effect, thus white gelatinous precipitate of aluminium hydroxide would be formed and slightly soluble in excess of the ammonia reagent. Therefore, in the case of the preparation of 'alumina–zirconia nanocomposite powder' from the aqueous solutions of aluminium and zirconium with the addition of the 25% concentrated ammonia

solution, the complete reactions were assumed to be as follows [26]:

$$Al(NO_3)_3{\cdot}9H_2O_{(aq)} + 3NH_4OH_{(l)} \rightarrow Al(OH)_{3(whitesol)} + 3NH_4NO_{3(l)} + 9H_2O_{(l)};\quad \text{thepHwascondition7} \quad (3)$$

$$ZrOCl_2{\cdot}8H_2O_{(aq)} + 2NH_4OH_{(l)} \rightarrow Zr(OH)_{4(whitessol)} + 2NH_4Cl_{(l)} + 7H_2O_{(l)};\quad \text{thepHwascondition7} \quad (4)$$

The reaction occurs step by step and slowly, based on the addition of ammonia.

The presence of sugar in the preparation significantly reduces the tendency toward agglomeration in the as-synthesized alumina–zirconia nanocomposite particles. The sugar has a sucrose structure, which contains hydroxyl and ether groups, whose hydrogen bond with the hydroxyl groups from the particle surfaces (Fig. 3). As a result, the surface hydroxyl groups get capped with the sugars. The sugar molecule coating on $Al_2O_3{\cdot}ZrO_2$ particle surfaces results in reduced particle aggregation due to the steric hindrance provided by the sugars.

The sugar has a sucrose structure, a disaccharide consisting of two monosaccharides of the six-carbon sugars D-glucose and D-fructose joined covalently by an O-glycosidic bond (See in Fig. 3). Sucrose can be considered a polyalcohol, because each monomer unit has hydroxyl groups, which can react to form alcohol derivatives [29].

The addition of a sugar template is important in the preparation of an alumina–zirconia nanocomposite. The crystal or particle size produced from the aluminium–zirconium salts will be smaller with the sugar template present. This is because the concentration of Al^{3+} and Zr^{4+} ions in the precursor will be lower over the course of the phase transformation with a certain amount of sugar. As the calcination temperature is increased, the material is considered to be so deficient in Al^{3+} and Zr^{4+} contents that it retards the crystallite grain growth. Furthermore, with an excess sugar concentration, this masking compound will be completely distributed across the salt surfaces, such that the binding distance or particle density will increase because sugar restricts the grain contact among the nucleated α-$Al_2O_3{\cdot}ZrO_2$ and restrains crystallite growth [30].

Quantitative analyses of the difractogram patterns, including the crystallite sizes of the alumina and zirconia phases formed, were performed for each sample using XRD software. The

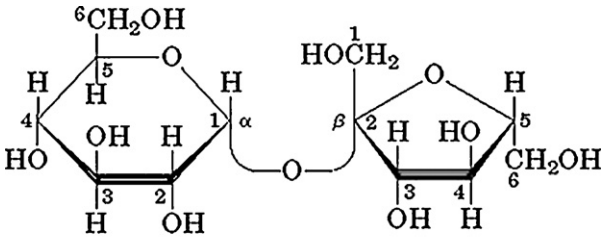

Fig. 3. The sucrose structure of sugar [29].

Scherrer equation was implemented to calculate the crystallite sizes of the zirconia and alumina phases in a sample at every calcination temperature, based on the main peaks of the XRD patterns from Figs. 1 and 2 [31].

$$D = \frac{K\lambda}{\beta \cos\theta} \quad (5)$$

where D is the crystallite size, K is a shape factor with a value of 0.9–1.4, λ is the wavelength of the X-rays (1.54056 Å), θ is Bragg's angle and β is the value of the full width at half maximum (FWHM). Table 3 presents the quantitative results of the alumina–zirconia nanocomposites at every calcination temperature, of any phases formed, using the Scherrer method. When the peak in an XRD pattern is broader with a lower intensity, the crystallite size is decreasing. By contrast, if the peak of an XRD pattern is becoming sharper, the crystallite size will be bigger and its crystallinity will be better. This trend is in agreement with the XRD patterns of the alumina–zirconia nanocomposite in Figs. 1 and 2.

3.2. Microstructures

Fig. 4 shows typical TEM bright field images of the alumina–zirconia nanocomposites at calcining temperatures of 800 °C (4a1,a2) and 1100 °C (4b) using a TECNAI G2-200 kV Phillips transmission electron microscope. The darker grains in these micrographs represent the zirconia phase and the lighter ones belong to the alumina phase (see in Fig. 4a1) [16]. The rather complex grains obtained from the sample calcined at 800 °C for 5 h (Fig. 4a2) were found to be related to the presence of two zirconia phases (m- and t-zirconia) along with the cubic γ-Al_2O_3 phase, in agreement with our XRD results in Fig. 1. The average grain sizes of the alumina and zirconia phases in the case of the sample calcined at 800 °C for 5 h were less than 25 nm. A rapid growth rate of alumina crystallites was exhibited at the point when the γ-Al_2O_3 phase transformed to the α-Al_2O_3 phase between 900 °C and 1000 °C (see in Table 3, the crystallite sizes of the zirconia and alumina phases in a sample at every calcination temperature), thus producing larger α-Al_2O_3 crystallites, 53 nm in size. By comparison, a slower growth rate was detected for m-ZrO_2 crystallites between 800 °C and 1100 °C. The average sizes of the t-ZrO_2 crystallites were 24, 31, 39 and 47 nm for the samples calcined at 800 °C, 900 °C, 1000 °C, and1100 °C, respectively. The observation of slower crystallite growth in the case of m-ZrO_2 could be related to the reduction of surface enthalpy in this phase, which can

Table 3
Quantitative results from the Scherrer method of the alumina and zirconia phases formed in alumina–zirconia nanocomposites.

No.	Mineral phase	Average crystallite size (nm)					PDF no.
		T800°C	T900°C	T1000°C	T1100°C	T1200°C	
1.	m-ZrO_2	24	31	39	47	54	83-0944
2.	t-ZrO_2	26	28	40	34	33	80-2156
3.	y-AI_2O_3	6	6	14	0	0	10-0425
4.	a-AI_2O_3	0	0	53	54	58	83-2080

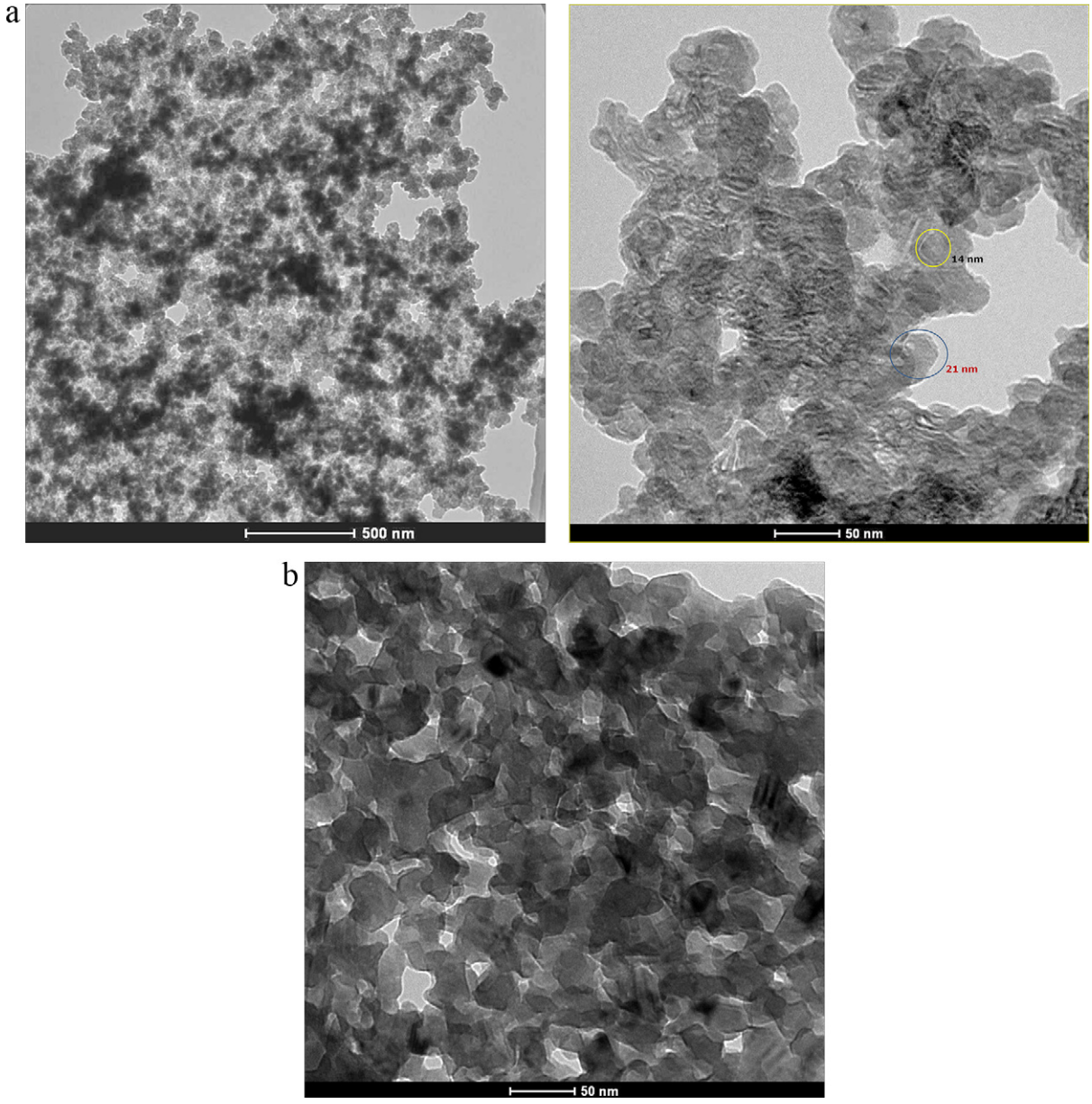

Fig. 4. TEM bright field images of the alumina–zirconia nanocomposite calcined at 800 °C (a1,a2), and 1100 °C (b) for 5 h.

give rise to slower sintering kinetics and grain growth rates during the calcination process [16]. Furthermore, the average grain sizes of the zirconia phases and the α-alumina phase for the samples calcined at 1100 °C for a fixed soaking time of 5 h were below 50 nm, as shown by the TEM in Fig. 4b.

Fig. 4(a2) and (b) shows transmission electronic microscopy images of the alumina–zirconia nanocomposite powder in which an appreciable formation of agglomerates after thermal treatment at 800 °C and 1100 °C can be seen. Fine particles, particularly nanoscale particles, because they have large surface areas, often agglomerate to form either lumps or secondary particles to minimize the total surface area or interfacial energy of the system. The agglomeration refers to the adhesion of the particles to each other because of van der Waals forces of attraction, which are significantly higher in nanoparticles [32].

3.3. Particle size distribution

Fig. 5 shows a typical particle size distribution of the alumina–zirconia nanocomposites calcined at 800 °C for 5 h, showing a size range of 10–40 nm with an average particle size (x50) of 20 nm. According to the histogram and the values for the cumulative distribution in Fig. 5, the largest nanocomposite particles had a size of about 40 nm and accounted for 3.49% of the total, while the mode value of the particle size distribution for these alumina–zirconia nanocomposites was 10 nm (0.01 μm), and those accounted for about 39.87% of the total. The particle sizes of the alumina–zirconia nanocomposites

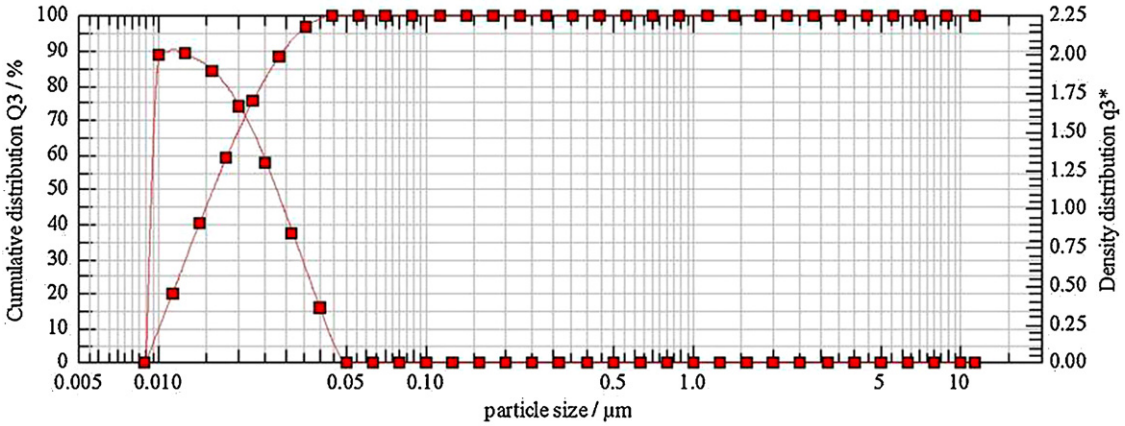

cumulative distribution

x_0/µm	Q_3/%	x_0/µm	Q_3/%	x_0/µm	Q_3/%	x_0/µm	Q_3/%
0.01	19.88	0.07	100.00	0.45	100.00	2.82	100.00
0.01	39.87	0.09	100.00	0.56	100.00	3.55	100.00
0.02	58.79	0.11	100.00	0.71	100.00	4.47	100.00
0.02	75.35	0.14	100.00	0.89	100.00	5.62	100.00
0.03	88.25	0.18	100.00	1.12	100.00	7.08	100.00
0.04	96.51	0.22	100.00	1.41	100.00	8.91	100.00
0.04	100.00	0.28	100.00	1.78	100.00	11.22	100.00
0.06	100.00	0.35	100.00	2.24	100.00		

histogram

x_m/µm	ΔQ_3/%	x_m/µm	ΔQ_3/%	x_m/µm	ΔQ_3/%	x_m/µm	ΔQ_3/%
0.01	19.88	0.06	0.00	0.40	0.00	2.51	0.00
0.01	19.99	0.08	0.00	0.50	0.00	3.16	0.00
0.02	18.92	0.10	0.00	0.63	0.00	3.98	0.00
0.02	16.56	0.13	0.00	0.79	0.00	5.01	0.00
0.03	12.90	0.16	0.00	1.00	0.00	6.31	0.00
0.03	8.27	0.20	0.00	1.26	0.00	7.94	0.00
0.04	3.49	0.25	0.00	1.58	0.00	10.00	0.00
0.05	0.00	0.32	0.00	2.00	0.00		

Fig. 5. Particle size distribution (determined by a SYMPHATEC NIMBUS particle size analyzer) of the alumina–zirconia nanocomposites calcined at 800 °C for 5 h.

calcined at 800 °C had a narrow distribution range, suggesting that, the particles of the alumina–zirconia nanocomposites have good uniformity.

The crystallite size is the size of a single crystal inside the particles or grains, whereas a single particle or grain can be composed of several crystals. The crystallite size is usually measured from X-ray diffraction patterns by the Scherrer method and particle or grain size by other experimental techniques like transmission electron microscopy (TEM). A particle itself consists of a larger single crystal or several crytals, thus TEM technique could be used to verify and to validate the crystallite sizes and shapes inside a particle. Nevertheless, particle size analysis is usually used to define the relative amounts of particles present in a material, sorted according to size, or it is also known as particle size distribution (PSD). At 800 °C, the crystallite sizes of the alumina–zirconia nanocomposites which theoretically calculated using the Scherrer method were estimated ranging from 6 to 26 nm; and this result was validated and verified by TEM analysis, which showing the average grain sizes of the alumina–zirconia nanocomposites calcined at 800 °C for 5 h were below 25 nm. However, particle size analysis measured the largest nanocomposite particles as having a size of about 40 nm, this could be meant that the largest nanocomposite particles composed of several crystals of γ-alumina, or combination of γ-alumina and t-/m-zirconia crystals or several crystals of t- and or m-zirconia.

The experimental results indicate that the overall process represents an effective and low cost methodology.

4. Conclusions

For the synthesis process of the alumina–zirconia nanocomposites, sugar was used as a gelling agent, and calcination was conducted at a lower temperature than was achieved by previous researchers. Alumina–zirconia nanocomposites were obtained at 800 °C, where the phases formed were γ-Al_2O_3, m-ZrO_2, and t-ZrO_2. The TEM results showed that the average grain sizes of the nanocomposite were less than 25 nm in diameter. At 800 °C, particle size analysis measured the largest nanocomposite particles as having a size of about 40 nm, accounting for 3.49% of the total, while the most common size was about 10 nm, accounting for 39.87% of the total. A further phase transformation of the nanocomposite was obtained at 1100 °C, where the phases formed were α-Al_2O_3, m-ZrO_2, and t-ZrO_2; and the TEM results showed the average grain sizes of the nanocomposite as having diameters below 50 nm.

Appendix A. Supplementary data

Supplementary data associated with this article can be found, in the online version, at doi:10.1016/j.ceramint.2011.05.086.

References

[1] J.A. Rodriguez, M.F. Garcia, Synthesis, Properties and Applications of Oxide Nanomaterials, 685, Willey Interscience, New Jersey, 2007, 692.
[2] Y. Lee, Y.M. Hahm, D.-H. Lee, Optimum conditions to prepare spherical alumina powder with controlled agregation under the W/O emulsion method, J. Ind. Eng. Chem. 10 (5) (2004) 826–833.
[3] W.H. Gitzen, Alumina as a ceramic material, American Ceramic Society, Columbia, Ohio, 1970p.43.
[4] D. Ganguli, M. Chatterjee, Ceramic Powder Preparation: A Handbook, Kluwer Academic Publishers, Boston, 1997, p75.
[5] M. Chartterjee, M.K. Naskar, D. Ganguli, Sol-emulsion-gel synthesis of alumina–zirconia composite microspheres, J. Sol–Gel Sci. Technol. 28 (2003) 217–225.
[6] W. Pyda, Nano-ceramic aspect of preparation and processing of zirconia nanopowders, Mater. Sci. Poland 26 (2) (2008) 403–412.
[7] D. He, Y. Ding, H. Luo, C. Li, Effects of zirconia phase on the synthesis of higher alcohols over zirconia and modified zirconia, J. Molec. Catal. A: Chem. 208 (2004) 267–271.
[8] S. Park, J.M. Vohs, R.J. Gorte, Direct oxidation of hydrocarbons in a solid-oxide fuel cell, Nature 404 (2000) 265–267.
[9] K.C. Patil, M.S. Hedge, T. Rattan, S.T. Aruna, Chemistry of Nanocrystalline Oxide Materials: Combustion synthesis, properties and applications, World Scientific, ISBN-13 978-981-279-314-0, New Jersey, 2008, p. 235.
[10] D.J. Green, Critical microstructures for microcracking in Al_2O_3–ZrO_2 composites, J. Am. Ceram. Soc. 65 (12) (1982) 610–614.
[11] B. Fegley Jr., P. White, H.K. Bowen, Preparation of zirconia–alumina powders by zirconium alkoxide hydrolysis, J. Am. Ceram. Soc. 68 (2) (1985) C60–C62.
[12] W.H. Tuan, R.Z. Chen, T.C. Wang, C.H. Cheng, P.S. Kuo, Mechanical properties of Al_2O_3/ZrO_2 composites, J. Eur. Ceram. Soc. 22 (2002) 2827–2833.
[13] R. Gadow, F. Kern, Presureless sintering of injection molded zirconia toughened alumina nano composites, J. Ceram. Soc. Jpn. 114 (11) (2006) 958–962.
[14] H. Jia, X. Liu, T. Li, H. Yan, B. Xu, Nickel and zirconia toughened alumina prepared by hydrothermal processing, J. Mater. Sci. 42 (2007) 4707–4711.
[15] H.S. Nalwa, Nanostructured Materials and Nanotechnology, Academic Press, London, 2002.
[16] A. Beitollahi, H. Hosseini-Bay, H. Sarpoolaki, Synthesis and characterization of Al_2O_3–ZrO_2 nanocomposite powder by sucrose process, J. Mater. Sci.: Mater. Electron. 21 (2010) 130–136.
[17] R. Caruso, O. Sanctis, A. Macias-Gracia, E. Benavidez, S.R. Mintzer, Influence of pH value and solvent utilized in the sol–gel synthesis on properties of derived ZrO_2 powders, J. Mater. Proc. Technol. 152 (2004) 299–303.
[18] H. Sheng-Wei, Y. Jian-Chang, Z. Si-En, Synthesis and characterization of alumina doped nano-ZrO_2 by surfactant-assisted route, Chin. J. Struct. Chem. 25 (5) (2006) 552–556.
[19] M.L. Balmer, F.F. Lange, V. Jayaram, C.G. Levi, Development of nanocomposite microstructures in Al_2O_3–ZrO_2 via the solution precursor method, J. Am. Ceram. Soc. 78 (6) (1995) 1489–1494.
[20] J.F. Bartolome, A.H. De Aza, A. Martın, J.Y. Pastor, J. Llorca, R. Torrecillas, G. Brunoz, Alumina/zirconia micro/nanocomposites: a new material for biomedical applications with superior sliding wear resistance, J. Am. Ceram. Soc. 90 (10) (2007) 3177–3184.
[21] F. Kern, G. Wadow, Extrusion and injection molding of ceramic micro and nanocomposites, Int. J. Mater. Forum 2 (1) (2009) 609–612.
[22] R.D. Purohit, S. Saha, A.K. Tyagi, Combustion synthesis of nanocrystalline ZrO_2 powder: XRD, Raman spectroscopy and TEM studies, Mater. Sci. Eng.: B 130 (1-3) (2006) 57–60.
[23] Y. Murase, E. Kato, K. Diamon, Stability of ZrO_2 phases in ultrafine ZrO_2–Al_2O_3 mixtures, J. Am. Ceram. Soc. 69 (2) (1986) 83–87.
[24] K. Ishida, K. Hirota, O. Yamaguchi, H. Kume, S. Inamura, H. Miyamoto, Formation of zirconia solid solutions containing alumina prepared by new preparation method, J. Am. Ceram. Soc. 77 (5) (1994) 1391–1395.
[25] S. Kikkawa, A. Kijima, K. Hirota, O. Yamamoto, Crystal structure of zirconia prepared with alumina by coprecipitation, J. Am. Ceram. Soc. 85 (3) (2002) 721–723.
[26] G. Shevla, 5th ed., Vogel's textbook of macro and semimicro qualitative inorganic analysis, 250, Longman Inc., New York, 1979, 39-48 535.
[27] C.J. Brinker, G.W. Scherer, Sol–Gel Science: The Physics and Chemistry of sol–gel processing, Academic Press Inc., San Diego, 1990, 21–26.
[28] T.C.W. Mak, Refinment of the crystal structure of zirconyl chloride octahydrate, Can. J. Chem. 46 (1968) 3491–3497.
[29] D.L. Nelson, M.M. Cox, Lehninger's Principles of Biochemistry, 4th ed., W.H. Freeman & Co., New York, 2004, p. 246.
[30] Y.C. Lee, S.-B. Wen, L. Wenglin, Nano α-Al_2O_3 powder preparation by calcining an emulsion precursor, J. Am. Ceram. Soc. 90 (2) (2007) 407–411.
[31] Y.J. Kwon, K.H. Kim, C.S. Lim, K.B. Shim, Characterization of ZnO nanopowders synthesized by the polymerized complex method via an organochemical route, J. Ceram. Proc. Res. 3 (2002) 146–149.
[32] V. Santos, M. Zeni, C.P. Bergmann, J.M. Hohemberger, Correlation between thermal treatment and tetragonal/monoclinic nanostructured zirconia powder obtained by sol–gel process, Rev. Adv. Mater. Sci. 17 (2008) 62–70.